Unlocking Asymmetric Michael Additions in an Archetypical Class I Aldolase by Directed Evolution

Kunzendorf, Andreas; Xu, Guangcai; Van Der Velde, Jesse J. H.; Rozeboom, Henriëtte J.; Thunnissen, Andy-mark W. H.; Poelarends, Gerrit J.

Published in:
ACS Catalysis

DOI:
10.1021/acscatal.1c03911

Publication date:
2021

ACS Catalysis

pubs.acs.org/acscatalysis

Research Article

Unlocking Asymmetric Michael Additions in an Archetypical Class I Aldolase by Directed Evolution

Andreas Kunzendorf,[§] Guangcai Xu,[§] Jesse J. H. van der Velde, Henriëtte J. Rozeboom, Andy-Mark W. H. Thunnissen, and Gerrit J. Poelarends*

Cite This: *ACS Catal.* 2021, 11, 13236–13243

Read Online

ACCESS | Metrics & More | Article Recommendations | Supporting Information

ABSTRACT: Class I aldolases catalyze asymmetric aldol addition reactions and have found extensive application in the biocatalytic synthesis of chiral β-hydroxy-carbonyl compounds. However, the usefulness of these powerful enzymes for application in other C−C bond-forming reactions remains thus far unexplored. The redesign of class I aldolases to expand their catalytic repertoire to include non-native carboligation reactions therefore continues to be a major challenge. Here, we report the successful redesign of 2-deoxy-D-ribose-5-phosphate aldolase (DERA) from *Escherichia coli*, an archetypical class I aldolase, to proficiently catalyze enantioselective Michael additions of nitromethane to α,β-unsaturated aldehydes to yield various pharmaceutically relevant chiral synthons. After 11 rounds of directed evolution, the redesigned DERA enzyme (DERA-MA) carried 12 amino-acid substitutions and had an impressive 190-fold enhancement in catalytic activity compared to the wildtype enzyme. The high catalytic efficiency of DERA-MA for this abiological reaction makes it a proficient "Michaelase" with potential for biocatalytic application. Crystallographic analysis provides a structural context for the evolved activity. Whereas an aldolase acts naturally by activating the enzyme-bound substrate as a nucleophile (enamine-based mechanism), DERA-MA instead acts by activating the enzyme-bound substrate as an electrophile (iminium-based mechanism). This work demonstrates the power of directed evolution to expand the reaction scope of natural aldolases to include asymmetric Michael addition reactions and presents opportunities to explore iminium catalysis with DERA-derived catalysts inspired by developments in the organocatalysis field.

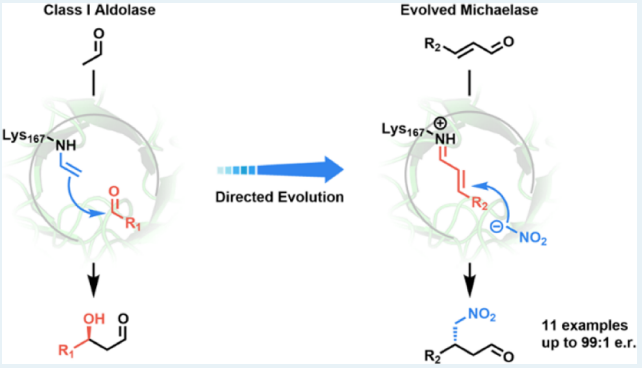

KEYWORDS: *aldolase, asymmetric catalysis, iminium biocatalysis, carboligation, directed evolution*

INTRODUCTION

Aldolases have evolved as powerful enzymatic tools in nature to reversibly catalyze aldol reactions, which provide an efficient synthetic strategy for asymmetric carbon−carbon bond assembly.[1,2] The aldol reaction usually utilizes an enolizable aldehyde or ketone as the nucleophilic donor substrate (aldol donor), which reacts with a second aldehyde or ketone acting as the electrophilic acceptor (aldol acceptor). Convergent evolution produced two mechanistically distinct aldolase classes,[3] each having a triosephosphate isomerase (TIM) barrel fold containing the active site. Class I aldolases utilize the ε-amino group of a highly conserved lysine to activate the aldol donor through the covalent formation of a Schiff base, followed by generating a highly nucleophilic enamine species. Instead, in class II aldolases, a metal ion cofactor (typically Zn^{2+}) acts as a Lewis acid and activates the aldol donor via coordination to the carbonyl group, facilitating deprotonation and enolate formation.[2] Found in eukaryotes, bacteria, and archaea, aldolases facilitate the reversible formation or cleavage of various carbohydrates, amino acids, and keto acids in essential metabolic pathways.[1,3]

The archetypical class I aldolase 2-deoxy-D-ribose-5-phosphate aldolase (DERA) catalyzes the reversible aldol addition between acetaldehyde (aldol donor) and D-glyceraldehyde-3-phosphate (aldol acceptor) to yield 2-deoxy-D-ribose-5-phosphate (Scheme 1a). In this reaction, Lys-167 acts as the conserved Schiff base-forming residue in the active site of DERA.[4] Although DERA accepts several small aldehydes and ketones such as propionaldehyde, acetone, and fluoroacetone as aldol donors,[5,6] the enzyme's limited nucleophile scope restricts its broader application.[7] In addition, DERA's catalytic efficiency for nonphosphorylated aldol acceptors is severely

Received: August 27, 2021
Revised: October 2, 2021
Published: October 15, 2021

Scheme 1. DERA-Catalyzed Carboligation Reactions via Enzyme-Bound Enamine or Iminium Ion Intermediates[a]

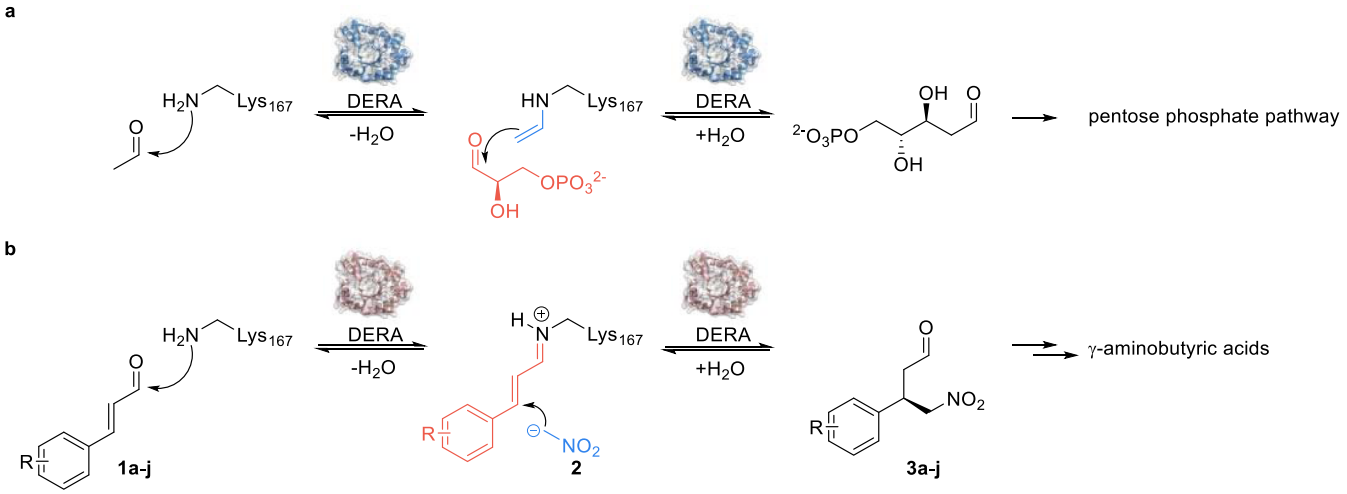

[a](a) DERA-catalyzed aldol addition of acetaldehyde to D-glyceraldehyde-3-phosphate to yield 2-deoxy-D-ribose-5-phosphate. The enzyme-bound substrate is activated as a nucleophilic enamine intermediate. (b) DERA-catalyzed Michael addition of nitromethane **2** to α,β-unsaturated aldehydes **1a**−**j** to produce γ-nitroaldehydes **3a**−**j**. The enzyme-bound substrate is activated as an electrophilic iminium ion intermediate. The participating nucleophilic donor substrate is highlighted in blue, whereas the electrophilic acceptor substrate is highlighted in red. Cartoon and surface presentation of DERA (PDB: 1JCL).

reduced[5,6] and enzyme inactivation at industrially relevant acetaldehyde concentrations[8] further limits DERA's efficient application. In the past, some of these limitations have been overcome by protein engineering[8−12] or novel protein discovery,[13−15] and over the past 20 years, DERA has found extensive application in the biocatalytic synthesis of chiral β-hydroxy-carbonyls. The industrial-scale application of engineered DERAs in processes developed by DSM[8,16] and Codexis/Merck[11] further underscore DERA's tremendous synthetic potential. However, to the best of our knowledge, the application of DERA in mechanistically related carboligations such as Morita−Baylis−Hillman,[17,18] Michael,[19,20] Mannich,[21] Knoevenagel,[22] and Henry-type[23] reactions remains so far unexplored. The development of efficient biocatalysts for such carboligations is pivotal because natural enzymes catalyzing these powerful carbon−carbon bond-forming reactions are rare.[24] Elucidating such novel catalytic activities within natural aldolases such as DERA would successfully expand the catalytic repertoire of the well-studied class I aldolase superfamily and offer new opportunities to develop synthetic useful biocatalytic applications.

Here, we report the successful redesign of DERA from *Escherichia coli* to efficiently catalyze asymmetric Michael additions of nitromethane to α,β-unsaturated aldehydes to produce enantiopure γ-nitroaldehydes, which are important chiral synthons for pharmaceutically active γ-aminobutyric acids.[25] After 11 rounds of directed evolution, the redesigned DERA enzyme (named DERA-MA) carried 12 amino-acid substitutions and had an impressive 190-fold enhancement in catalytic activity compared to the wildtype enzyme. High-resolution crystal structures of DERA-MA in a substrate-free and substrate-bound state revealed how some of the mutations reshaped the substrate-binding pocket at the active site for accommodating the α,β-unsaturated aldehyde and directing it toward the catalytic lysine, resulting in the formation of a covalent Schiff-base intermediate. These results demonstrate the power of directed evolution to enlarge the reaction scope of an archetypical class I aldolase to include asymmetric Michael additions and present new opportunities to develop a family of novel DERA-derived catalysts for several mechanistically related carboligations.

RESULTS AND DISCUSSION

Identifying Novel Carboligation Reactions Catalyzed by DERA. While DERA from *E. coli* has been extensively explored for aldol additions in biocatalytic processes developed by academia and industry, the question remains whether this enzyme can be used to promote mechanistically related carboligation reactions such as synthetically useful Michael additions. Considering that the active site of DERA can accommodate various aldehydes, we started our investigations by testing if DERA can serve as a catalyst in the asymmetric synthesis of valuable γ-nitroaldehydes. These important chiral synthons for abundantly prescribed pharmaceuticals can be prepared through either a Michael-type addition of acetaldehyde to α,β-unsaturated nitroalkenes or a Michael addition of nitromethane to α,β-unsaturated aldehydes.[19,20] First, we examined whether DERA is able to use its natural donor substrate acetaldehyde (50 and 150 mM) in the Michael-type addition to the non-native acceptor substrate *trans*-nitrostyrene (2 mM) but could not observe any substrate conversion with the wildtype enzyme. Next, we tested whether DERA can catalyze the Michael addition of nitromethane **2** to cinnamaldehyde **1a** (Scheme 1b). This reaction was performed in the presence of wildtype DERA (DERA-wt, 17.4 μM) in sodium phosphate buffer (pH 6.5) containing 3% v/v DMSO, 2 mM **1a**, and 20 mM **2**. Remarkably, DERA displayed catalytic activity with these non-native substrates, and monitoring the reaction progress by GC−MS analysis showed that the desired γ-nitroaldehyde **3a** was produced with 38% conversion after 30 h (Figure S1a). Analysis of product **3a** by chiral GC further indicated that DERA afforded the pharmaceutically relevant *R*-enantiomer of **3a** with good enantiopurity (e.r. = 96:4; Figure S1b). Notably, under otherwise identical reaction conditions, a reaction without DERA or with the variant DERA K167L, in which the active

https://doi.org/10.1021/acscatal.1c03911
ACS Catal. 2021, 11, 13236−13243

site Lys-167 has been replaced with a leucine,[4] afforded only trace amounts of product **3a**. Hence, the active site of DERA can give rise to synthetically useful catalytic promiscuity, utilizing Lys-167 as a key catalytic residue to promote the Michael addition of **2** to **1a** to give enantioenriched *R*-**3a**, albeit with low-level activity.

Directed Evolution of DERA. Motivated by these initial findings, we set out to develop an efficient directed evolution strategy for the optimization of DERA for the Michael addition of **2** to **1a**. With the intention of randomly sampling the sequence space of DERA for beneficial mutations, we used error-prone PCR in the first round of our directed evolution campaign. To reduce the total screening effort, the resulting library (~75,000 bacterial colonies) was first analyzed for active DERA mutants using a prescreening assay termed as activated iminium colony staining (AICS), which relies on the complexation of 2-hydroxycinnamaldehyde with the active site Lys-167 of DERA, forming a brightly red-colored merocyanine-dye-type structure.[26] Bacterial colonies that formed this red-colored species upon incubation with 2-hydroxycinnamaldehyde proved to express DERA variants with a substantial activity for the Michael-type addition of **2** to **1a**, whereas bacterial colonies that showed no staining by 2-hydroxycinnamaldehyde expressed DERA-wt or mutants that exhibited no or very low-level activity. Stained colonies (about 0.1% of the library) were selected, and subsequent UV−vis-based activity assays with the recovered DERA variants revealed several mutants that displayed significantly improved activity for the Michael-type addition of **2** to **1a**, with the best variant showing a ~9.5-fold enhanced activity over DERA-wt.

Having established the effectiveness of our directed evolution strategy to enhance the Michael addition activity of DERA, we subsequently optimized DERA for this unnatural activity by combining gene shuffling of DERA variants possessing beneficial mutations,[27] site-saturation mutagenesis of active-site residues, and random mutagenesis using either error-prone PCR[28] to target the whole protein sequence or spiked oligonucleotides to target strand−helix connecting loops surrounding the active site.[29] After 11 rounds of directed evolution, we obtained a DERA variant (named DERA-MA) with an impressive 190-fold enhancement in catalytic activity compared to that of DERA-wt (Figures 1; S2, see Supporting Information for a rationale and schematic overview of the directed evolution campaign). This DERA variant contains 12 amino-acid substitutions, 8 of which were introduced by random mutagenesis using error-prone PCR (T18S, D22G, D24Y, C47S, F52S, T197S, A203T, and S239G), 2 by cassette mutagenesis with spiked oligonucleotides (K172L and V206A), and 2 by site-saturation mutagenesis (P202V and T142S). Importantly, throughout the laboratory evolution process, the enantioselectivity of DERA also improved enabling production of the desired product **3a** with an excellent e.r. of 99:1 (*R*/*S*).

Characterization of DERA-MA. In order to assess the catalytic performance of DERA-MA, we determined steady-state kinetic parameters using varying concentrations of **1a** in the presence of a saturating concentration (100 mM) of **2** (Figures S3 and S28). Optimization of DERA by directed evolution for the Michael addition of **2** to **1a** resulted in an apparent k_{cat} ($k_{cat,app}$) of 0.38 ± 0.01 s^{-1} and a $K_{M,app}$ of 302 ± 14 μM ($k_{cat,app}/K_{M,app}$ = 1258 s^{-1} M^{-1}). Impressively, DERA-MA displayed a 100-fold higher activity for the Michael addition of **2** to **1a** compared to a previously engineered 4-

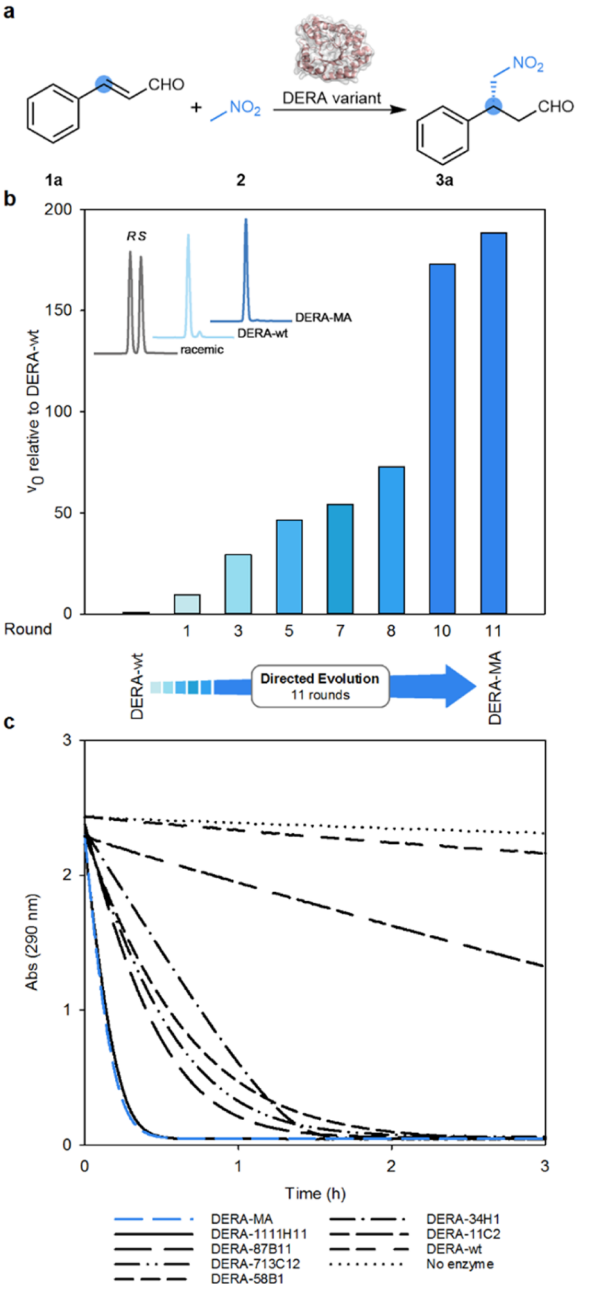

Figure 1. Directed evolution of DERA. (a) DERA was optimized by directed evolution for the Michael addition of nitromethane **2** to cinnamaldehyde **1a**, yielding γ-nitroaldehyde **3a**. (b) Comparison of the Michael addition activity of DERA-wt and engineered DERA variants. Initial rates (v_0) are given relative to the initial rate of the reaction catalyzed by DERA-wt, and they were measured by UV−vis spectroscopy with 5 μM DERA, 1 mM **1a**, and 100 mM **2** (n = 2). The inset shows the stereoselectivity of DERA-wt and DERA-MA, as detected by chiral GC. (c) Reaction progress curves of different DERA variants corresponding to the variants shown in panel (b).

oxalocrotonate tautomerase (4-OT) variant.[30] Whereas the symmetry relationship within homohexameric 4-OT, with any point mutation reflected in all six subunits, imposes a significant limitation for its optimization, the TIM barrel fold architecture of DERA proved to be more susceptible for enzyme optimization, yielding a proficient "Michaelase" (DERA-MA) with potential for biocatalytic application. Notably, the original retro-aldolase activity with the natural

https://doi.org/10.1021/acscatal.1c03911
ACS Catal. 2021, 11, 13236−13243

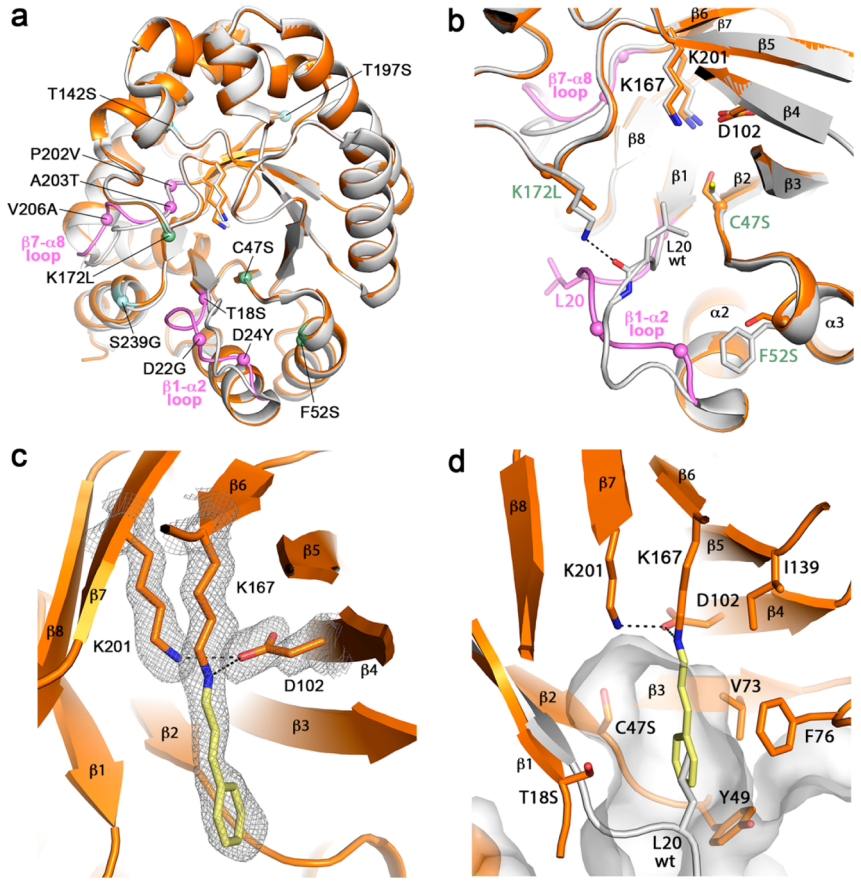

Figure 2. Crystal structures and active site of DERA-MA. (a) Overlay of the overall structures of apo-DERA-MA (orange, PDB entry 7P7S) and DERA-wt (light grey, PDB entry 1P1X) in cartoon representation. The 12 mutations in the DERA-MA polypeptide chain are indicated as spheres. Loops β1-α2 and β7-α8 in DERA-MA (pink) display significant conformational differences relative to DERA-wt. The largest conformational change is observed for the β1-α2 loop and is likely influenced by surrounding mutations C47S, F52S, and K172L (green). (b) Closeup view of the active-site regions of DERA-MA and DERA-wt, displaying the conformational difference of the β1-α2 loop and the large displacement of Leu-20 from an inward (DERA-wt) to outward (DERA-MA) position. (c) Active site in cinnamaldehyde-soaked DERA-MA (PDB entry 7P76), showing the covalent Schiff-base intermediate of Lys-167 with cinnamylidene (yellow) in stick representation. Also shown are the side chains of conserved active-site residues Asp-102 and Lys-201. The gray mesh represents the 1.9 Å electron density for the three active-site residues and cinnamylidene adduct ($2F_o$–F_c Fourier omit map, contoured at 1σ). (d) Cinnamylidene-binding pocket in DERA-MA (PDB entry 7P76), showing the Schiff-base intermediate together with the side chains of surrounding residues. The β1-α2 loop and Leu-20 side chain of DERA-wt are also shown as an overlay in light gray. The phenyl ring of the cinnamylidene moiety is located at a position which in DERA-wt is occupied by the side chain of Leu-20. The molecular surface in gray defines the boundaries of the active-site pocket in DERA-MA.

substrate 2-deoxy-D-ribose-5-phosphate is lost in DERA-MA, which indicates that the newly gained catalytic function for Michael additions comes at the expense of the original activity (Figure S6).

Replacing Lys-167 with a leucine (DERA-MA K167L) gives a more than 150-fold reduction in catalytic activity, indicating that Lys-167 is crucial for the Michael addition activity of DERA-MA (Figure S5). This suggests that Lys-167 retains its important catalytic function as the Schiff base-forming residue in the DERA-MA catalyzed Michael addition of **2** to **1a**. Further evidence for formation of an iminium ion between Lys-167 and **1a** during the catalytic cycle is provided by the appearance of a new bathochromic absorbance peak for **1a** at 350 nm in the presence of DERA-MA (Figure S7). In contrast, no bathochromic shift was detected upon incubation of **1a** with DERA-MA K167L. Similar bathochromic shifts in substrate absorbance have been observed for other iminium ion-forming organocatalysts[31] and enzymes.[26,32] Spectroscopic titration studies with a Schiff-base adduct of **1a** in organic solvents[33] suggest that the species formed between **1a** and Lys-167 is likely protonated. Additionally, after chemically reducing DERA-MA in the presence of **1a** with $NaBH_3CN$, ESI-MS analysis revealed that compared to unmodified DERA-MA, the observed major peak increased by + 117 Da, corresponding to the covalent modification of the protein with one molecule of the reduced Schiff-base adduct of **1a** (calcd. 28760.8 Da; found, 28761.0 Da; Figure S8). To gain further insights into the position of modification, the modified and unmodified DERA-MA samples were digested with endoproteinase Glu-C and the resulting peptide mixtures analyzed by LC–MS/MS. A comparison of the detected peptide fragments of DERA-MA modified with **1a** to those of unmodified DERA-MA showed that peptides that contain the Lys-167 residue are the major sites of modification (mass increase of +116 Da; Tables S3 and S4). Together, these results strongly suggest that Lys-167 activates **1a** by forming an iminium ion, which is followed by a nucleophilic attack of **2** (upon deprotonation) to form a new carbon–carbon bond.

The evolved DERA-MA variant contains 12 amino-acid substitutions compared to the wildtype enzyme. To investigate

https://doi.org/10.1021/acscatal.1c03911
ACS Catal. 2021, 11, 13236–13243

Table 1. Enantioselective Synthesis of γ-Nitroaldehydes Using DERA-MA as a Biocatalyst

a Substrate scope[a]

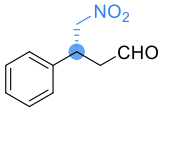

3a 1 h, >95 % conv. 99:1 e.r.

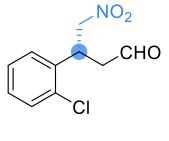

3b 1 h, >95 % conv. 99:1 e.r.

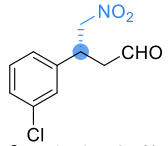

3c 1.5 h, >95 % conv. 99:1 e.r.

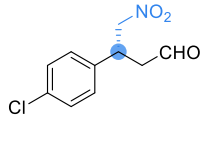

3d 2 h, >95 % conv. 99:1 e.r.

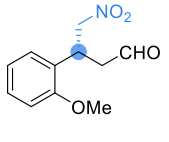

3e 10 h, >95 % conv. 86:14 e.r.

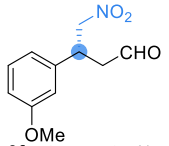

3f 2.5 h, >95 % conv. 97:3 e.r.

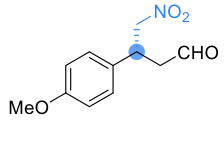

3g 8 h, >95 % conv. 91:9 e.r.

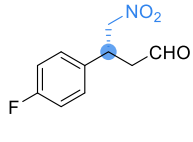

3h 1 h, >95 % conv. 99:1 e.r.

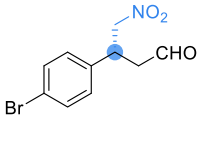

3i 1.5 h, >95 % conv. 99:1 e.r.

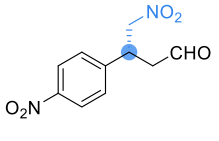

3j 2 h, >95 % conv. 99:1 e.r.

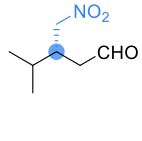

3k 24 h, 53 % conv. 82:18 e.r.[b]

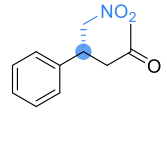

3l Not detected

b Semi-preparative scale[c]

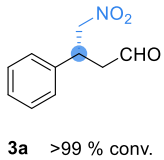

3a >99 % conv. 66 % yield 99:1 e.r.

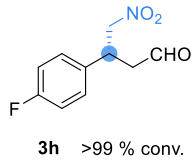

3h >99 % conv. 65 % yield 99:1 e.r.

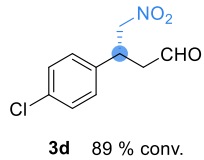

3d 89 % conv. 56 % yield 99:1 e.r.[d]

Precursor:	Phenibut	Fluorophenibut	Baclofen

[a]Analysis of substrate scope with 1 mM **1a–l**, 20 mM **2**, and 5 μM DERA-MA in 20 mM HEPES, 100 mM NaCl, pH 6.5, 3% v/v DMSO at 29 °C. Reaction times determined after UV–vis analysis indicated consumption of **1a–l**, conversions determined by GC-FID, enantiomeric ratios determined by chiral HPLC/GC. [b]Reaction progress followed by GC–MS. [c]Semipreparative-scale reactions with 5 mM **1a**,**d**,**h**, 20 mM **2**, and 4 μM DERA-MA in 10 mM HEPES, 100 mM NaCl, pH 6.5, 3% v/v DMSO at 29 °C. Conversions determined by ^{1}H NMR analysis, yields are isolated yields, enantiomeric ratios determined by chiral HPLC. [d]Performed with 8 μM DERA-MA.

the contribution of each of these new amino acid residues to the Michael addition activity of DERA-MA, we constructed 12 enzyme variants in which each residue in DERA-MA was sequentially replaced by the corresponding amino acid in the wildtype enzyme. Two of these back-mutations (S47C and T203A) resulted in an over fourfold reduced activity of DERA-MA (Figure S5). Additionally, eight back-mutations showed a somewhat lower but still significant effect on the activity of DERA-MA, whereas two back-mutations (G22D and S197T) had no influence on activity. Overall, this indicates that most of the amino-acid substitutions in DERA-MA (10 out of 12), mainly introduced by random mutagenesis approaches, benefit the optimization of the enzyme's non-natural Michael addition activity.

Structural Analysis of DERA-MA. To gain insights into the structural consequences of the introduced mutations, we solved high-resolution crystal structures of DERA-MA in a substrate-free state, as well as in a covalent reaction intermediate state obtained by briefly soaking crystals with the substrate cinnamaldehyde (Figures 2, S9 and S10, Table S5). The overall structure of DERA-MA is almost identical to that of wildtype DERA (the root-mean-square deviation for Cα-backbone atoms is ~0.8 Å), displaying the typical $(\alpha/\beta)_8$ (TIM-barrel) fold with the catalytic Lys-167 located at the C-terminal end of strand β6. The catalytic lysine is in close proximity to the side chains of conserved Lys-201 (strand β7) and Asp-102 (strand β4), two additional residues with crucial roles in the native catalytic mechanism of DERA.[4,34] A total of 10 of the 12 mutations are located in 5 strand–helix-connecting loops at the C-terminal side of the TIM-barrel surrounding the active-site region (Figure 2a). These are T18S, D22G, and D24Y in loop β1-α2, C47S and F52S in loop β2-α3, K172L in loop β6-α7, P202V, A203T and V206A in loop β7-α8, and S239G in loop β8-α9. The mutation T142S is also located at the C-terminal side of the TIM-barrel but in the secondary shell of the active site, whereas mutation T197S is

https://doi.org/10.1021/acscatal.1c03911
ACS Catal. 2021, 11, 13236–13243

located on the other side of the TIM-barrel outside of the active site. Two loops, β1-α2 and β7-α8, each containing three mutations, display a significant change in backbone conformation compared to the wildtype structure (Figure 2a,b). The most prominent difference is observed for the β1-α2 loop, which changes from an inward-facing conformation in the wildtype structure (with respect to the active-site region) to an outward-facing conformation in the structure of DERA-MA (in some of the unique protein molecules in the DERA-MA crystals, the loop is disordered). The conformational difference of the β1-α2 loop is influenced by three nearby mutations in the DERA-MA structure (i.e., C47S, F52S, and K172L), which disrupt some of the favorable interactions that stabilize the loop in the wildtype structure (Figure 2b). Notably, in the DERA-wt structure, Cys-47 forms a hydrophobic contact with the side chain of Leu-20 in the β1-α2 loop. In the DERA-MA structure, this latter residue has been pulled out from the active-site area, opening a hydrophobic pocket lined by the side chains of Tyr-49, Val-73, and Phe-76. In the structure obtained by soaking a DERA-MA crystal with cinnamaldehyde, we observed extra electron density connected to the side chain of Lys-167, consistent with the formation of a covalent Schiff-base intermediate (Figure 2c). The extra electron density allowed us to unambiguously define the binding mode of the Lys-167-linked cinnamylidene moiety, showing that it is firmly bound with its phenyl ring in the hydrophobic pocket that in DERA-wt is occupied by Leu-20 (Figure 2d). The crystal structures thus explain how some of the mutations, in particular C47S, enable the Michael addition activity of DERA-MA, by helping to create a new pocket in the active site for binding cinnamaldehyde and allowing the terminal carbonyl to be attacked by the ε-amino group of Lys-167, thereby forming the Schiff-base intermediate. The structure/function relationships of the other mutation that is crucial for the Michael addition activity of DERA-MA, A203T in the β7-α8 loop, are less clear. In wildtype DERA, the β7-α8 loop participates in binding 2-deoxy-D-ribose-5-phosphate and stabilizing the Schiff-base intermediate formed between Lys-167 and the natural substrate in the retro-aldol reaction.[4] From our structural comparison, it appears that in DERA-MA, the Thr-203 side chain sterically hinders binding of 2-deoxy-D-ribose-5-phosphate (Figure S9a). Furthermore, the movement of the β7-α8 loop away from the active site precludes the formation of a favorable hydrogen bond with the phosphate group of 2-deoxy-D-ribose-5-phosphate, together explaining why DERA-MA does not display any retro-aldolase activity with the natural substrate. How the A203T mutation contributes to enhancing the Michael addition activity of DERA-MA is uncertain, but possibly, the threonine side chain helps to direct the terminal carbonyl of cinnamaldehyde toward the ε-amino group of Lys-167. We expect that the Schiff-base intermediate formed between Lys-167 and cinnamaldehyde is stabilized via electron resonance, resulting in a partial positive charge on the C3 carbon of the cinnamylidene moiety, which would favor attack by nitromethane, which is activated as a nucleophile by deprotonation. The DERA-MA crystal structure of the Schiff-base complex with cinnamaldehyde reveals that the C3 carbon is indeed easily accessible for such an attack from its *re*-face, while the *si*-face is blocked due to contacts with Val-73 and Phe-76, thus explaining the stereochemistry of the overall reaction (Figures S9b,c,d and S10).

Substrate Scope of DERA-MA. With the optimized enzyme DERA-MA in hand, we assessed its synthetic performance for the Michael addition of **2** to a variety of α,β-unsaturated aldehydes **1a**−**k** and α,β-unsaturated ketone **1l** (Table 1a). In addition to **1a**, DERA-MA readily accepts aldehydes **1b**−**d** with electron-withdrawing substitutions in the *ortho*-, *meta*-, or *para*-position as non-native substrates. The sterically more demanding aldehydes **1e**−**g** with electron-donating substitutions in the *ortho*-, *meta*-, or *para*-position are equally accepted as substrates, albeit with a slight decrease in catalytic activity and stereoselectivity. *Para*-substituted aldehydes **1h**−**j** are also efficiently processed by DERA-MA. The enzymatic products **3a**−**j** were obtained with good conversions (>95%) as the desired *R*-enantiomers with good to excellent enantiopurity (e.r. = 86:14 − 99:1). Hence, DERA-MA shows a broad substrate scope, accepting various cinnamaldehydes with electron-donating or electron-withdrawing substitutions on the aromatic ring. The aliphatic unsaturated aldehyde **1k** was also accepted as a non-native substrate by DERA-MA but with moderate conversion and decreased stereoselectivity compared to the aromatic α,β-unsaturated aldehydes **1a**−**j**. Notably, the α,β-unsaturated ketone **1l** was not accepted as a substrate by the evolved enzyme, illustrating the preference of DERA-MA for α,β-unsaturated aldehydes.

Finally, we further demonstrated the synthetic usefulness of DERA-MA by performing semipreparative-scale synthesis of selected γ-nitroaldehydes (*R*-**3a**,**d**,**h**). High conversions (89 to >99%), excellent enantiopurity (e.r. = 99:1) and good isolated product yields (up to 66%) were achieved (Table 1b). Notably, *R*-**3a**,**d**,**h** are valuable synthetic precursors that can be easily converted to the pharmaceutically active γ-aminobutyric acids phenibut,[35] baclofen,[36] and fluorophenibut,[37] respectively, by two simple steps.[38]

CONCLUSIONS

Natural aldolases are regarded as highly specific for their nucleophilic aldol donor[7] and are restricted by the range of reactions catalyzed. Even though the substrate scope, activity, and stability[8−12,39] of the archetypical class I aldolase DERA have been successfully altered to enlarge its usefulness for diverse aldol reactions, examples of other mechanistically related carboligation reactions catalyzed by DERA are unknown. In the current study, we demonstrate that the active site of DERA from *E. coli* can give rise to synthetically useful catalytic promiscuity, supporting asymmetric Michael additions of nitromethane to various α,β-unsaturated aldehydes to give γ-nitroaldehydes, important chiral synthons for pharmaceutically active γ-aminobutyric acids. Using directed evolution, we have successfully demonstrated that this promiscuous Michael addition activity of DERA can be enhanced 190-fold, yielding a new enantioselective biocatalyst (DERA-MA) with unprecedented catalytic efficiency for a challenging abiological carbon−carbon bond-forming reaction. Biochemical and structural analysis of DERA-MA supports a reaction mechanism that involves Schiff base formation between the ε-amino group of Lys-167 and the non-natural cinnamaldehyde substrate, activating it for attack by (deprotonated) nitromethane at the *re*-face of the cinnamylidene C3 carbon, explaining the *R*-enantioselective formation of γ-nitroaldehydes. Interestingly, we found that 10 of the 12 mutations in DERA-MA are located in strand−helix-connecting loops at the C-terminal side of the TIM-barrel, surrounding the active-site region. This suggests that targeting loops close to the active

https://doi.org/10.1021/acscatal.1c03911
ACS Catal. 2021, 11, 13236−13243

site of DERA will be an efficient strategy to engineer this enzyme for other functions as well.

These results demonstrate the power of directed evolution to expand the limited catalytic repertoire of a natural class I aldolase to include asymmetric Michael addition reactions. While an aldolase acts naturally by activating the enzyme-bound substrate as a nucleophile (i.e., an enamine-based mechanism), DERA-MA on the other hand acts by activating the enzyme-bound substrate as an electrophile (i.e., an iminium-based mechanism). Hence, via iminium catalysis, DERA-MA could possibly accelerate many of the bond-forming reactions promoted by organocatalysts,[20,40] presenting new opportunities to develop a family of DERA-derived catalysts for various mechanistically related and synthetically useful transformations, including carboligations. In this context, it is important to emphasize that during the evolution of one new catalytic activity, additional and potentially useful functions can emerge within an enzymatic active site.[41] Indeed, our directed evolution program has generated a versatile set of novel DERA variants that might serve as promising stepping stones to further evolve new catalytic functions, such as mechanistically related Mannich,[21] Knoevenagel,[22] Henry,[23] and Morita−Baylis−Hillman[17,18] reactions. Current work in our group focuses on elucidating alternative substrates (e.g., haloalkanes, diethyl (halo)malonates, cyanide, hydroperoxides, amines, and thiols) and new catalytic activities for these evolved DERA variants to further enlarge the catalytic repertoire of DERA-derived catalysts for the synthesis of valuable chiral building blocks. The high-throughput AICS assay, followed by medium-throughput activity assays with different cinnamaldehydes and nucleophilic donor substrates, also proved to be successful for the engineering of DERA variants for efficient asymmetric synthesis of enantioenriched α,β-epoxy-aldehydes and substituted chroman-2-ols. These preliminary results will be reported in due course. It is important to emphasize that the AICS assay mainly detects DERA variants capable of forming an electrophilic iminium ion intermediate with cinnamaldehydes. Hence, activity screening with different pairs of electrophilic and nucleophilic donor substrates will require the use of alternative high-throughput screening assays.

■ ASSOCIATED CONTENT

Supporting Information

The Supporting Information is available free of charge at https://pubs.acs.org/doi/10.1021/acscatal.1c03911.

Experimental procedures and compound characterization (PDF)

■ AUTHOR INFORMATION

Corresponding Author

Gerrit J. Poelarends − *Department of Chemical and Pharmaceutical Biology, Groningen Research Institute of Pharmacy, University of Groningen, 9713 AV Groningen, The Netherlands;* orcid.org/0000-0002-6917-6368; Phone: +31503633354; Email: g.j.poelarends@rug.nl, http://www.rug.nl/staff/g.j.poelarends/

Authors

Andreas Kunzendorf − *Department of Chemical and Pharmaceutical Biology, Groningen Research Institute of Pharmacy, University of Groningen, 9713 AV Groningen, The Netherlands*

Guangcai Xu − *Department of Chemical and Pharmaceutical Biology, Groningen Research Institute of Pharmacy, University of Groningen, 9713 AV Groningen, The Netherlands*

Jesse J. H. van der Velde − *Department of Chemical and Pharmaceutical Biology, Groningen Research Institute of Pharmacy, University of Groningen, 9713 AV Groningen, The Netherlands*

Henriëtte J. Rozeboom − *Molecular Enzymology Group, Groningen Biomolecular Sciences and Biotechnology Institute, University of Groningen, 9747 AG Groningen, The Netherlands*

Andy-Mark W. H. Thunnissen − *Molecular Enzymology Group, Groningen Biomolecular Sciences and Biotechnology Institute, University of Groningen, 9747 AG Groningen, The Netherlands;* orcid.org/0000-0002-1915-9850

Complete contact information is available at: https://pubs.acs.org/10.1021/acscatal.1c03911

Author Contributions

§A.K. and G.X. contributed equally to the work.

Notes

The authors declare no competing financial interest.

■ ACKNOWLEDGMENTS

We thank M.H. de Vries for support in acquiring mass spectrometry data and beamline staff at the European Synchrotron Radiation Facility MASSIF-1 for help with X-ray diffraction data collection. We acknowledge financial support from the Netherlands Organisation of Scientific Research (VICI grant 724.016.002).

■ REFERENCES

(1) Samland, A. K.; Sprenger, G. A. Microbial aldolases as C-C bonding enzymes-unknown treasures and new developments. *Appl. Microbiol. Biotechnol.* **2006**, *71*, 253−264.

(2) Clapés, P.; Garrabou, X. Current Trends in Asymmetric Synthesis with Aldolases. *Adv. Synth. Catal.* **2011**, *353*, 2263−2283.

(3) Marsh, J. J.; Lebherz, H. G. Fructose-Bisphosphate Aldolases: An Evolutionary History. *Trends Biochem. Sci.* **1992**, *17*, 110−113.

(4) Heine, A.; DeSantis, G.; Luz, J. G.; Mitchell, M.; Wong, C.-H.; Wilson, I. A. Observation of Covalent Intermediates in an Enzyme Mechanism at Atomic Resolution. *Science* **2001**, *294*, 369−374.

(5) Barbas, C. F.; Wang, Y. F.; Wong, C. H. Deoxyribose-5-Phosphate Aldolase as a Synthetic Catalyst. *J. Am. Chem. Soc.* **1990**, *112*, 2013−2014.

(6) Chen, L.; Dumas, D. P.; Wong, C. H. Deoxyribose 5-Phosphate Aldolase as a Catalyst in Asymmetric Aldol Condensation. *J. Am. Chem. Soc.* **1992**, *114*, 741−748.

(7) Hernández, K.; Szekrenyi, A.; Clapés, P. Nucleophile Promiscuity of Natural and Engineered Aldolases. *ChemBioChem* **2018**, *19*, 1353−1358.

(8) Jennewein, S.; Schürmann, M.; Wolberg, M.; Hilker, I.; Luiten, R.; Wubbolts, M.; Mink, D. Directed Evolution of an Industrial Biocatalyst: 2-Deoxy-D-Ribose 5-Phosphate Aldolase. *Biotechnol. J.* **2006**, *1*, 537−548.

(9) DeSantis, G.; Liu, J.; Clark, D. P.; Heine, A.; Wilson, I. A.; Wong, C.-H. Structure-Based Mutagenesis Approaches toward Expanding the Substrate Specificity of D-2-Deoxyribose-5-Phosphate Aldolase. *Bioorg. Med. Chem.* **2003**, *11*, 43−52.

(10) Dick, M.; Hartmann, R.; Weiergräber, O. H.; Bisterfeld, C.; Classen, T.; Schwarten, M.; Neudecker, P.; Willbold, D.; Pietruszka, J. Mechanism-Based Inhibition of an Aldolase at High Concentrations

of Its Natural Substrate Acetaldehyde: Structural Insights and Protective Strategies. *Chem. Sci.* **2016**, *7*, 4492−4502.
(11) Huffman, M. A.; Fryszkowska, A.; Alvizo, O.; Borra-Garske, M.; Campos, K. R.; Canada, K. A.; Devine, P. N.; Duan, D.; Forstater, J. H.; Grosser, S. T.; Halsey, H. M.; Hughes, G. J.; Jo, J.; Joyce, L. A.; Kolev, J. N.; Liang, J.; Maloney, K. M.; Mann, B. F.; Marshall, N. M.; McLaughlin, M.; Moore, J. C.; Murphy, G. S.; Nawrat, C. C.; Nazor, J.; Novick, S.; Patel, N. R.; Rodriguez-Granillo, A.; Robaire, S. A.; Sherer, E. C.; Truppo, M. D.; Whittaker, A. M.; Verma, D.; Xiao, L.; Xu, Y.; Yang, H. Design of an in Vitro Biocatalytic Cascade for the Manufacture of Islatravir. *Science* **2019**, *366*, 1255−1259.
(12) Voutilainen, S.; Heinonen, M.; Andberg, M.; Jokinen, E.; Maaheimo, H.; Pääkkönen, J.; Hakulinen, N.; Rouvinen, J.; Lähdesmäki, H.; Kaski, S.; Rousu, J.; Penttilä, M.; Koivula, A. Substrate Specificity of 2-Deoxy-D-Ribose 5-Phosphate Aldolase (DERA) Assessed by Different Protein Engineering and Machine Learning Methods. *Appl. Microbiol. Biotechnol.* **2020**, *104*, 10515−10529.
(13) Chambre, D.; Guérard-Hélaine, C.; Darii, E.; Mariage, A.; Petit, J.-L.; Salanoubat, M.; de Berardinis, V.; Lemaire, M.; Hélaine, V. 2-Deoxyribose-5-Phosphate Aldolase, a Remarkably Tolerant Aldolase towards Nucleophile Substrates. *Chem. Commun.* **2019**, *55*, 7498−7501.
(14) Fei, H.; Zheng, C.-c.; Liu, X.-y.; Li, Q. An Industrially Applied Biocatalyst: 2-Deoxy-D-Ribose-5- Phosphate Aldolase. *Process Biochem.* **2017**, *63*, 55−59.
(15) Haridas, M.; Abdelraheem, E. M. M.; Hanefeld, U. 2-Deoxy-D-Ribose-5-Phosphate Aldolase (DERA): Applications and Modifications. *Appl. Microbiol. Biotechnol.* **2018**, *102*, 9959−9971.
(16) Wolberg, M.; Dassen, B. H. N.; Schürmann, M.; Jennewein, S.; Wubbolts, M. G.; Schoemaker, H. E.; Mink, D. Large-Scale Synthesis of New Pyranoid Building Blocks Based on Aldolase-Catalysed Carbon-Carbon Bond Formation. *Adv. Synth. Catal.* **2008**, *350*, 1751−1759.
(17) Morita, K.-i.; Suzuki, Z.; Hirose, H. A Tertiary Phosphine-Catalyzed Reaction of Acrylic Compounds with Aldehydes. *Bull. Chem. Soc. Jpn.* **1968**, *41*, 2815.
(18) Baylis, A. B.; Hillman, M. E. D. Verfahren Zur Herstellung von Acryl-Verbindungen. DE2155113A1, 1972.
(19) Mukherjee, S.; Yang, J. W.; Hoffmann, S.; List, B. Asymmetric Enamine Catalysis. *Chem. Rev.* **2007**, *107*, 5471−5569.
(20) Erkkilä, A.; Majander, I.; Pihko, P. M. Iminium Catalysis. *Chem. Rev.* **2007**, *107*, 5416−5470.
(21) Arend, M.; Westermann, B.; Risch, N. Modern Variants of the Mannich Reaction. *Angew. Chem., Int. Ed.* **1998**, *37*, 1044−1070.
(22) List, B. Emil Knoevenagel and the Roots of Aminocatalysis. *Angew. Chem., Int. Ed.* **2010**, *49*, 1730−1734.
(23) Luzzio, F. A. The Henry Reaction: Recent Examples. *Tetrahedron* **2001**, *57*, 915−945.
(24) Miao, Y.; Rahimi, M.; Geertsema, E. M.; Poelarends, G. J. Recent developments in enzyme promiscuity for carbon-carbon bond-forming reactions. *Curr. Opin. Chem. Biol.* **2015**, *25*, 115−123.
(25) Ordóñez, M.; Cativiela, C.; Romero-Estudillo, I. An Update on the Stereoselective Synthesis of γ-Amino Acids. *Tetrahedron: Asymmetry* **2016**, *27*, 999−1055.
(26) Biewenga, L.; Crotti, M.; Saifuddin, M.; Poelarends, G. J. Selective Colorimetric "Turn-On" Probe for Efficient Engineering of Iminium Biocatalysis. *ACS Omega* **2020**, *5*, 2397−2405.
(27) Zhao, H.; Zha, W. In vitro 'sexual' evolution through the PCR-based staggered extension process (StEP). *Nat. Protoc.* **2006**, *1*, 1865−1871.
(28) Leung, D. W.; Chen, E.; Goeddel, D. V. A Method for Random Mutagenesis of a Defined DNA Segment Using a Modified Polymerase Chain Reaction. *Technique* **1989**, *1*, 11−15.
(29) Hermes, J. D.; Parekh, S. M.; Blacklow, S. C.; Koster, H.; Knowles, J. R. A Reliable Method for Random Mutagenesis: The Generation of Mutant Libraries Using Spiked Oligodeoxyribonucleotide Primers. *Gene* **1989**, *84*, 143−151.
(30) Guo, C.; Saifuddin, M.; Saravanan, T.; Sharifi, M.; Poelarends, G. J. Biocatalytic Asymmetric Michael Additions of Nitromethane to α,β-Unsaturated Aldehydes via Enzyme-bound Iminium Ion Intermediates. *ACS Catal.* **2019**, *9*, 4369−4373.
(31) Silvi, M.; Verrier, C.; Rey, Y. P.; Buzzetti, L.; Melchiorre, P. Visible-light excitation of iminium ions enables the enantioselective catalytic β-alkylation of enals. *Nat. Chem.* **2017**, *9*, 868−873.
(32) Garrabou, X.; Wicky, B. I. M.; Hilvert, D. Fast Knoevenagel Condensations Catalyzed by an Artificial Schiff-Base-Forming Enzyme. *J. Am. Chem. Soc.* **2016**, *138*, 6972−6974.
(33) Jiménez-Sánchez, A.; Rodríguez, M.; Métivier, R.; Ramos-Ortíz, G.; Maldonado, J. L.; Réboles, N.; Farfán, N.; Nakatani, K.; Santillan, R. Synthesis and Crystal Structures of a Series of Schiff Bases: A Photo-, Solvato- and Acidochromic Compound. *New J. Chem.* **2014**, *38*, 730−738.
(34) Heine, A.; Luz, J. G.; Wong, C.-H.; Wilson, I. A. Analysis of the Class I Aldolase Binding Site Architecture Based on the Crystal Structure of 2-Deoxyribose-5-phosphate Aldolase at 0.99Å Resolution. *J. Mol. Biol.* **2004**, *343*, 1019−1034.
(35) Lapin, I. Phenibut (β-Phenyl-GABA): A Tranquilizer and Nootropic Drug. *CNS Drug Rev.* **2006**, *7*, 471−481.
(36) Olpe, H.-R.; Demiéville, H.; Baltzer, V.; Bencze, W. L.; Koella, W. P.; Wolf, P.; Haas, H. L. The biological activity of d-baclofen (Lipresal). *Eur. J. Pharmacol.* **1978**, *52*, 133−136.
(37) Bowery, N. G.; Hill, D. R.; Hudson, A. L. Characteristics of $GABA_B$ Receptor Binding Sites on Rat Whole Brain Synaptic Membranes. *Br. J. Pharmacol.* **1983**, *78*, 191−206.
(38) Biewenga, L.; Saravanan, T.; Kunzendorf, A.; van der Meer, J.-Y.; Pijning, T.; Tepper, P. G.; van Merkerk, R.; Charnock, S. J.; Thunnissen, A.-M. W. H.; Poelarends, G. J. Enantioselective Synthesis of Pharmaceutically Active γ-Aminobutyric Acids Using a Tailor-Made Artificial Michaelase in One-Pot Cascade Reactions. *ACS Catal.* **2019**, *9*, 1503−1513.
(39) Rouvinen, J.; Andberg, M.; Pääkkönen, J.; Hakulinen, N.; Koivula, A. Current State of and Need for Enzyme Engineering of 2-Deoxy-D-Ribose 5-Phosphate Aldolases and Its Impact. *Appl. Microbiol. Biotechnol.* **2021**, *105*, 6215−6228.
(40) Bertelsen, S.; Jørgensen, K. A. Organocatalysis-after the gold rush. *Chem. Soc. Rev.* **2009**, *38*, 2178.
(41) Khersonsky, O.; Tawfik, D. S. Enzyme Promiscuity: A Mechanistic and Evolutionary Perspective. *Annu. Rev. Biochem.* **2010**, *79*, 471−505.

https://doi.org/10.1021/acscatal.1c03911
ACS Catal. 2021, 11, 13236−13243